Lab on a Chip

Devices and applications at the micro- and nanoscale

Accepted Manuscript

View Article Online
DOI: 10.1039/D0LC00921K

Fangchao Yin, [a,d,1] Xu Zhang, [a,1] Li Wang, [e] Yaqing Wang, [a,d] Yujuan Zhu, [a,d] Zhongyu Li, [a] Tingting Tao, [a,d] Wenwen Chen, [a,d] Hao Yu, [a] and Jianhua Qin*[a,b,c,d]

[a] CAS Key Laboratory of SSAC, Department of biotechnology, Dalian Institute of Chemical Physics, Chinese Academy of Sciences.

[b] Institute for Stem Cell and Regeneration, Chinese Academy of Sciences, Beijing, China.

[c] CAS Center for Excellence in Brain Science and Intelligence Technology, Chinese Academy of Sciences, Shanghai, China.

[d] University of Chinese Academy of Sciences, Beijing, China.

[e] Institutes of Biomedical Sciences, Fudan University, Shanghai, China.

[1]These authors contribute equally to the work.

* Corresponding author: Prof. J. Qin, E-mail: jhqin@dicp.ac.cn

The poor predictive power of the existing preclinical models has spurred efforts to develop human relevant models for accurate assessment of drug safety. In this work, we developed a multi-organoids-on-a-chip system derived from human induced pluripotent stem cells (hiPSCs), which allows for the assessment of the cardiac safety of antidepressant drug, following liver metabolism . This liver-heart organoids on chip device contains compartmentalized chambers separated by porous membrane, which permits the co-culture of 3D human liver organoids (LOs) in the upper multi-well chamber and cardiac organoids (COs) in the bottom micropillar array simultaneously. The co-cultured liver and heart organoids on chip maintained good viability and human organ-specific functions respectively, including the synthesis of albumin and urea of liver organoids, and beating function of cardiac organoids. In particular, the liver organoids displayed proper metabolic capabilities with high expression of CYP450 enzyme genes. Clomipramine, a widely used antidepressant drug, can be metabolized into the active metabolite (desmethylclomipramine) through

the hepatic CYP450 enzymes of liver organoids on chip identified by mass spectrometry. After exposure to 1 μM clomipramine in the liver chamber for 24h and 48h, the co-cultured heart organoids in the bottom layer showed significantly reduced cell viability, impaired functions of cardiac beating and calcium flux, indicating the hepatic metabolism dependent cardiotoxicity induced by clomipramine. By combining stem cell biology and microengineered technology, this proposed hiPSC-derived multi-organoids chip system can reflect human organ-specific functions, as well as the complex process of drug metabolism and responses at the multi-organ level. It may provide a novel platform for the assessment of drug effectiveness and safety .

Clomipramine, human induced pluripotent stem cell, multi-organoids-on-chip, drug metabolism, heart-liver chip

Medications present safety challenges because it needs to balance the well-being of patients with potential side effect of drugs[1, 2]. Generally, only 5 in 10000 compounds can enter into the clinical trails and eventually 1 of them is approved by the Food and Drug Administration (FDA)[3, 4]. Drug-induced hepatic and cardiac side effects are main concerns for drugs failure from clinical trails and withdrawn from the market[5, 6]. The models that can accurately predict human outcomes of drug toxicity and the crosstalk between different organs are still lacking. Thus, the assessment of drug safety in a physiologically relevant manner may greatly contribute to guide the clinical usage of medications.

the pharmacokinetic process of drugs involves in absorption, distribution, metabolism and exclusion. Liver as a major organ of drug metabolism, greatly determines pharmacological properties of drugs, such as the bioavailability and adverse effects. Gain insight into the drug metabolism and safety may greatly contribute to increase the success rate of drug discovery and guide the clinical usage

View Article Online
DOI: 10.1039/D0LC00921K

of medication. However, the traditional preclinical models mainly rely on the two-dimensional (2D) monolayer cell cultures and animal experiments. Generally, the monolayer cell cultures are oversimplified to reflect the physiological conditions and xenobiotic metabolism of organs . Moreover, the single cell type cannot model the physiological complexity of inter-organ interactions and the process of drug pharmacokinetics. Although the animal models have been applied to assess the safety of antidepressants, they can hardly represent the human relevant responses to drugs due to the interspecies divergence[7]. Therefore, it is highly desirable to develop human relevant model for safety assessment of antidepressant.

Organoids are 3D cellular clusters by self-organization of pluripotent stem cells (PSCs) that are capable of recapitulating key features of native organs or tissues[8, 9]. Especially, human induced PSC (hiPSC)-derived organoids hold great potential for organ development studies, disease modeling and drug testing. Organoids-on-chip is emerging as an innovative technology by combining self-organized organoids and organs-on-chips to build higher-fidelity 3D organ models[10-13], thus potentially bridging the gap between monolayer cultures and animal models. The integrative strategies could be used for better produce the human organ models by precise control over the 3D culture, dynamic flow and mechanical cues in an organ chip device[14-16]. Recently, a series of organoid-on-a-chips have been successfully established, such as liver[17], brain[12], and islet[18] etc. The organoid-on-a-chip platform offers new frontiers and possibilities for applications in biomedicine.

In this work, we build a multi-organoids-on-chip system from hiPSCs for the safety assessment of antidepressant drug, for the first time. Clomipramine, a kind of FDA-approved tricyclic antidepressants for patients with severe depression[19, 20], was used as a model drug in this system. The bioengineered organoids chip system was designed with four layers that allowed the 3D co-culture of liver and heart organoids within the compartmentalized chambers after the formation of self-organized organoids from hiPSCs. The upper multi-well chamber allows the culture of liver

organoids for the metabolism of clomipramine, and the bottom micropillar array permits the differentiation and culture of heart organoids for the assessment of drug toxicity. The organ-specific genes expression and functions of the liver and cardiac organoids were identified in the co-culture system. Then the responses of heart organoids to clomipramine were investigated by examining the cardiac viability and functions in the presence and absence of hepatic metabolism. This human multi-organoids system derived from hiPSCs may provide a proof-of-concept for drug safety assessment in a physiologically relevant manner.

The device was fabricated using soft lithography techniques as previously described[21, 22]. The device consisted of four layers: a top layer, a ploy(dimethylsiloxane) (PDMS, Dow corning, USA) layer with 500 μm diameter through-hole, a transparent polycarbonate porous membrane with 0.4 μm pores (Whatman Corp, United Kingdom) and a bottom layer ( ). The top PDMS layer was fabricated with a culture channel (length: 15 mm, width: 5 mm and height: 1 mm). The bottom PDMS layer (length: 20 mm, width: 5 mm and height: 1 mm) consisted of an array of patterned micropillars (diameter: 500 μm and height: 700 μm) with gaps of 100 μm use for 3D culture of cardiac organoids. The three PDMS layers were generated by mixing the PDMS at weight ratio of 10:1 and curing at 80 ℃ for 30 min. The top PDMS layer was bonded to the through-hole PDMS membrane following oxygen plasma treatment. The polycarbonate porous membrane adhered to the surface of the bottom layer through the electrostatic interaction, then PDMS pre-polymer was smeared on the membrane. After curing, the through-hole PDMS membrane and transparent membrane were bonded together following the plasma treatment. Before the experiments, the chip devices were sterilized in an autoclave.

The hiPSC line was kindly provided by Dr. Ning Sun[23, 24]. Undifferentiated hiPSCs were cultured in mTeSR1 medium (STEMCELL Technologies, Canada) on

117

EBs. On day 0, the EBs were induced in RPMI 1640 medium adding with B27 minus insulin (50×, Gibco, USA) and glycogen synthase kinase 3 inhibitor CHIR99021 (12 μM, Selleck, USA). After 24 h, the medium was replaced with fresh RPMI 1640 medium containing B27 minus insulin. After 2 more days incubation, the medium was changed to RPMI 1640 medium with B27 minus insulin and Wnt inhibitor IWP2 (5 μM, Selleck, USA). On day 5, the culture medium was replaced with fresh RPMI 1640 medium with B27 minus insulin. On day 7, the cells were fed with RPMI 1640 medium containing B27 every 3 days. The beating cardiac organoids were observed at day 10-12 after differentiation.

The cardiac organoids were induced and grown in the bottom chamber of the chip for 20 days. The liver organoids were then seeded into the upper culture chamber. The medium was mixed at a ratio of 1:1 with RPMI 1640 medium containing B27 and HCM medium supplemented with 10^{-7} M dexamethasone, which was changed every day. After co-culturing for 7 days, clomipramine at different concentrations was added to the upper liver culture chamber for 24 h and 48 h.

The beating of cardiac tissue was recorded by real time video recording with a high-resolution CCD (Leica, Germany). Videos of beating cardiac organoids were then analyzed using motion tracking software as described before[26, 27]. Briefly, these beating cardiac organoids videos were transformed into a series of single-frame image files (10 frames/s) and then input to motion tracking software[26] for calculation.

Liver organoids and cardiac organoids for immunostaining were prepared as described in our previous work[17, 28]. Briefly, organoids were fixed with 4% paraformaldehyde for 20 min at room temperature. The fixed organoids were dehydrated by incubation with 30% sucrose solution overnight at 4 ℃. Organoids were embedded in O.C.T. compound (Sakura) and cryosectioned at 10 μm with a cryostat (Leica). The freezing sections were washed with PBS to remove excess

View Article Online
DOI: 10.1039/D0LC00921K

O.C.T. and permeabilized with 0.25% Triton X-100 for 10 min. Sections were blocked with goat serum (Solarbio, SL1) for 1h at room temperature, and then incubated with primary antibodies overnight at 4℃. Samples were washed with PBS three times and were then incubated with secondary antibodies for 1 h at room temperature. The fluorescent images were recorded using a confocal microscope (Olympus). Primary and secondary antibodies used here were listed in the .

The real-time PCR was performed as described in our previous study[11]. Briefly, the total RNA was extracted from the organoids or hiPSCs using Trizol reagent (TAKARA). Then, the RNA was reverse-transcribed to generate cDNA with PrimeScript RT Reagent Kit (Takara) and the concentrations of the RNA were measured by a NanoDrop spectrophotometer (Thermo, America) to ensure that we used same mass of mRNA (250 ng/ml) in each sample before the reverse transcription. Finally, quantitative PCR (qPCR) was performed on PikoReal 96 real-time PCR System (Thermo). The housekeeping gene (β-actin) was used as an internal control for normalization of all qPCR results. Primers were listed in .

Cell viability of human liver and heart organoids were examined after the incubation with 1 μM or 10 μM clomipramine for 24 h and 48 h using the CCK-8 kit (Cell Counting Kit-8, Dojindo). The experiments have been performed according to the manufacturer's instructions.

The media from the supernatant of liver organoids on chip were collected for urea measurement. The concentration of urea production in the medium was measured using a QuantiChrom urea assay kit (BioAssay Systems) according to the manufacturer.

After the drug treatment, cardiac organoids were incubated with Fluo-4 Direct™

View Article Online
DOI: 10.1039/D0LC00921K

Calcium reagent (Invitrogen) at 37 ℃ for 60 min. Afterwards, the reagent was removed and changed to RMPI 1640 medium. The videos of calcium sparks were recorded using a high-resolution CCD. Then the videos were exported as a series of PNG files for beating study using Adobe Premier Pro2017. The PNG files were analyzed using image-Pro Plus software to detect the fluorescence intensity changing over time as previously described[29]. ΔF/F0 was calculated to normalize differences of the indicator concentration between cells.

The stock solution of 10 mM clomipramine (clomipramine HCl, Selleck Chemicals) was prepared in H_2O. After 7 days of co-culture, 1 μM clomipramine was added to the medium in the upper chamber and metabolized for 24 h. Then, 500 μL of the supernatant was collected from the chamber and added to 100 μL acetonitrile and 500 μL sodium carbonate solution (1 mol L^{-1}), followed by mixing. The mixture was added to 3 mL n-hexane and then vortexed for 1 min, reciprocated for 15 min. After centrifuging at 4000 rpm for 15 min, the organic phase was transferred to a polyethylene tube and dried in a vacuum desiccator. The dried residue was re-dissolved in 200 μL acetonitrile and detected using an Agilent Ultra High Performance Liquid Chromatography-Mass Spectrometer (LC-MS, Agilent 1290 Infinity, 6540 UHD Q-TOF). Finally, 20 μL aliquots was injected into LC-MS for analysis of the drug metabolites.

All quantitative data were calculated from three independent experiments. Statistical significance was analyzed using Student's -test and present as mean±SD. * < 0.05, ** < 0.01, < 0.001 were determined to be significant.

In this study, we designed and fabricated a multi-organoids-on-chip device, which enabled to evaluate the drug-induced cardiac toxicity after its metabolism in liver

View Article Online
DOI: 10.1039/D0LC00921K

organoids ( ). This liver-heart organoids-on-chip device contains four layers, including the top layer, through-hole PDMS layer, polycarbonate porous membrane and bottom layer. The through-hole PDMS layer and the polycarbonate membrane formed the upper microwell chamber, which permitted the 3D culture of hiPSC-derived liver organoids. The bottom chamber with micropillar array allowed the controlled formation of EBs with consistent morphology, in situ differentiation and self-organization of heart organoids from hiPSCs. The microwell and micropillar structures facilitate the production of uniform organoids and avoid the fusion of organoids, thus reducing their variability. Moreover, the compartmentalized chip design is flexible and conductive to different ways of drug administration, organoids collection and downstream analysis. It is noted, the polycarbonate porous membrane sandwiched between the upper and lower layers can not only facilitate the interconnection of the media, drug metabolites diffusion and nutrients exchange, but also be amenable to real-time imaging of organoids on chip. As such, the established multi-organoids-on-chip is feasible to be applied for the subsequent co-culture of distinct organoids and the assessment of drug bioactivity and toxicity via organ-organ interactions.

To generate 3D cardiac organoids from hiPSCs on a chip, we used a defined differentiation protocol with chemicals and growth factors added into the medium. The hiPSC-derived EBs were initially generated on the micropillar array of bottom layer, following in situ sequential induction of the mesendoderm, cardiac specific mesoderm, cardiomyocytes and organization of cardiac organoids (. Generally, the spontaneous contraction occurs at day 10 to day 12 after differentiation. To evaluate the features of cardiac organoids differentiation, we examined the expression of cardiac-specific genes by real-time PCR ( ). As expected, the expression of cardiac-specific markers (cTnT and TNNT3) significantly increased on day 20 compared to the hiPSC control, while the expression of the pluripotent markers of stem cells decreased . Moreover, the expression of

cardiac transcriptional factor (NKX2.5) was detected at markedly high levels in heart organoids. To further identify the maturity of cardiac organoids, the immunohistochemical analysis of cardiac-specific markers was performed in organoids ( ). The results showed an abundant expression of cTnT in cardiac organoids on day 20. These data validated the efficient differentiation of cardiac organoids from hiPSCs in our device.

The liver organoids were generated from hiPSC-derived EBs, followed by endoderm differentiation, hepatic progenitor induction and maturation using a three-stage differentiation protocol ( ). To examine the differentiation of liver organoids, the expressions of pluripotent markers of stem cells and hepatic lineage markers were tested by real-time PCR. The expression of pluripotent markers (OCT4 and NANOG) decreased , which suggests the differentiation of hiPSCs. While the hepatic progenitor (AFP) and mature hepatocyte (ALB and HNF4α) markers were significantly upregulated in liver organoids on 20 days of differentiation ( ). Moreover, the immunohistochemical analysis showed a higher expression of ALB and cytochrome P450 (CYP3A4) in organoids on day 20 , indicating the representative metabolic function of the liver organoids. These results suggested the efficient differentiation of hiPSCs into hepatic lineages and the formation of liver organoids.

Multi-organs-on-chip system enables the modeling of the crosstalk among organs, holding great potential to investigate the systemic diseases and pharmacology. To evaluate the cardiac safety of antidepressants administration following liver metabolism, we integrated the liver and cardiac organoids on a multilayered chip device to enable the co-culture of these organoids. The cardiac organoids were differentiated from hiPSCs in the bottom layer of the device for 20 days, then liver organoids were infused into the upper chamber. To verify the feasibility of the integrated microphysiological system, the functional characterizations of the co-cultured human cardiac and liver organoids were identified. At first, the urea

production of liver organoids in the co-culture system was examined to assess the liver-specific function. As shown in urea production was markedly increasing at day 3 and 7 of co-culture. Moreover, the liver organoids exhibited significantly increased expressions of liver-specific CYP450 enzyme genes (CYP3A4 and CYP1A2) on day 7. The expressions of other metabolic enzyme genes, such as CYP2C19 and CYP2D6, in liver organoid co-cultured with cardiac organoid were similar to that in liver organoid cultured alone ( ). These data suggested that liver organoids displayed favorable specific functions in this integrated system.

In addition, the cardiomyocytes specific functions including beating rate and velocity were measured in cardiac organoids from day 1 to day 7 in the presence or absence of liver organoids. As shown in and , the cardiac organoids in co-culture system displayed no significant differences in terms of spontaneous beat frequency and maximum beating velocities in comparison with single cultures. Compared with previous work that reported the increasing heart rate when co-culture with hepatocytes[30], the stable functions of cardiac tissue here may benefit from the 3D structure of organoid, which is more physiological morphology. Besides, the organoids in the chip exhibited good uniformity that could increase the stability of functions as well. Overall, cardiac and liver organoids maintained their tissue-specific functions in the co-culture system over 7 days, reflecting that this liver-heart model could might be available to assess drug cardiotoxicity following liver metabolism.

Liver plays a crucial role in the substance metabolism and detoxification . CYP450 enzymes are vital drug metabolizing enzymes in human liver. Four typical cytochrome enzymes, CYP1A2, CYP2C19, CYP2D6 and CYP3A4, have been found to be closely related to the clomipramine metabolism[31] ( ). Specifically, clomipramine is hydroxylized to hydroxyclomipramine by CYP2D6, then demethylated to desmethylclomipramine by CYP2C19, CYP3A4, and finally converted to hydroxydesmethylclomipramine by CYP2D6. To assess the metabolic

capacity of liver organoids, we examined the expression of CYP1A2, CYP2C19, CYP2D6 and CYP3A4 using real-time PCR. As shown in , all four drug metabolism-related CYP450 enzymes were significantly upregulated in the liver organoids on day 20, demonstrating the potential metabolic capacity of liver organoids. Furthermore, to verify the drug metabolism by the liver organoids, 1 μM clomipramine was introduced to the liver organoids for 24 h. Then the supernatant was collected to identify the production of metabolites with LC-MS/MS. As shown in , clomipramine with m/z 315 and desmethylclomipramine with m/z 301 were detected (top of). Notably, the peak of desmethylclomipramine (m/z 301) was observed only in the spectrogram after its metabolism in liver organoids ( ). Moreover, the characteristic peaks of secondary mass spectrograms (bottom of) double confirmed the presence of these two compounds. These data suggested that hiPSC-derived liver organoids possessed the metabolic ability to metabolize clomipramine into desmethylclomipramine, which accurately recapitulated the clomipramine metabolism .

Prior to examine the safety of clomipramine on cardiac tissues, we initially evaluated the toxic effect of antidepressant on liver organoids. Clinically, the plasma drug concentration of clomipramine in patients is 50 600ng/ml (0.16-1.90 uM)[32] and its active metabolite desmethylclomipramine exceeding a certain concentration (~1.43 μM) might lead to an increase in adverse reactions[33, 34]. Thus, the day-20 liver organoids were exposed to a physiological relevant concentration of clomipramine (1 μM) and high dose of the drug (10 μM) for the treatment at different time periods (24 h and 48 h). As shown in , liver organoids showed no significant changes of cell viability after 1 μM clomipramine exposure compared to the control group, while a decrease of cell viability with 10 μM clomipramine treatment for 48 h. Similarly, the liver-specific functions, such as the urea synthesis in liver organoids was markedly decreased with a high dose of clomipramine treatment . These

results revealed that the high dose of clomipramine caused significantly damages of cell viability and liver-specific functions, consisting with other reports or clinical results.

To further explore the effects of clomipramine on the cardiac tissues following liver metabolism, a low concentration of clomipramine (1 μM) was administered into the integrated multi-organoids system. In this system, clomipramine and its metabolites could diffuse to the bottom channel with cardiac organoids. After exposed to 1 μM clomipramine for 24 h or 48 h in liver organoids, the cell viability of cardiac organoids was initially examined to evaluate the drug-induced cardiotoxicity. The data showed that clomipramine triggered significant cell death of cardiac organoids, regardless of the presence or absence of liver organoids . Moreover, the effects of clomipramine administration on cardiac-specific functions, including the beating rate and beating velocity of cardiac organoids were examined under different culture conditions. The results showed that clomipramine can lead to reduced cardiac beating rate and beating velocity from 20 μm/s to10 μm/s in the co-culture system ( ), indicating that the clomipramine-induced cardiotoxicity dependent on liver metabolism. Calcium flux plays an important role in cardiac electrical activity and directly activates the myofilaments, causing contractions. The concentration of free intracellular Ca^{2+} oscillates during the cardiac action potential[35]. To monitor the intracellular calcium influx, we used Fluo-4 AM to indicate the calcium handling of cardiac organoids under different culture conditions. As shown in , cardiac organoids exhibited lower levels of cytosolic Ca^{2+} after treatment with 1 μM clomipramine. Moreover, clomipramine could reduce the release of calcium flux in cardiac tissue in co-culture systems, further proving the significant cardiotoxicity induced by clomipramine metabolites. As we know, Tricyclic antidepressants (TCAs) are highly lipid soluble drugs, which can pass through placenta, accumulate in utero, and cause congenital malformations of fetus. The proposed multi-organoids-on-a-chip system may have the potential to integrate with the maternal-fetal barrier and probe the effects of clomipramine and its metabolites on cardio-development in the future.

View Article Online
DOI: 10.1039/D0LC00921K

The pharmacokinetic-pharmacodynamic (PK-PD) analysis can be applied on this system, which provides an important guideline for dosage selection and drug assessment[36, 37].

Herein, we proposed a new multi-organoids-on-chip system from hiPSCs that allowed to assess the safety of antidepressants on cardiac tissue following liver metabolism. This device contained compartmentalized chambers enables the differentiation and 3D co-culture of functional liver and heart organoids simultaneously. In this model, the administration of antidepressant clomipramine at a low concentration led to the increased cardiotoxicity in heart organoids after its metabolism in liver organoids, including the decreased cell viability, cardiac contractility and calcium flux in heart organoids. These results showed the hepatic metabolism-dependent toxic responses of this drug in cardiac tissue, revealing the feasibility of this human multi-organoids chip system for predicting the side effects of this antidepressant drug.

This work provides the proof-of-concept to develop hiPSC-derived multi-organoids-on-chip by combining developmental biology principle and bioengineered technology. The human organoids chip system enables to mimic the multiorgan physiology by 3D co-culture of liver and heart organoids and facilitates the assessment of drug safety in a physiological relevant manner. It could reflect the multiple process of drug metabolism and responses at the multi-organ level , which provides a novel platform for drug effectiveness and toxicity assessment.

This research was supported by the National Science and Technology Major Project (No. 2018ZX09201017-001-001), the Strategic Priority Research Program of the Chinese Academy of Sciences, Grant (No. XDB32030200, XDB29050301, XDA16020900,), National Nature Science Foundation of China (No. 81703470, 81803492, 31971373), Innovation Program of Science and Research from the DICP,

View Article Online
DOI: 10.1039/D0LC00921K

406 CAS (DICP I201934).

407

408 The authors declare no competing financial interests.

View Article Online
DOI: 10.1039/D0LC00921K

1. P. Molero, J. A. Ramos-Quiroga, R. Martin-Santos, E. Calvo-Sanchez, L. Gutierrez-Rojas and J. J. Meana, *CNS Drugs*, 2018, **32**, 411-420.

2. A. Z. Antosik-Wojcinska, B. Stefanowski and L. Swiecicki, *Psychiatr Pol*, 2015, **49**, 1223-1239.

3. S. D. Kim, G. Kang, J. M. Kim, J. H. Ryu, K. C. Kim, H. S. Kwon, K. H. Kim, H. K. Lee and S. W. Song, *Journal of Pharmacological and Toxicological Methods*, 2017, **88**, 198-199.

4. W. J. Crumb, Jr., J. Vicente, L. Johannesen and D. G. Strauss, *J Pharmacol Toxicol Methods*, 2016, **81**, 251-262.

5. J. E. B. J. D. o. t. F. S. Randles, 1947, **1**.

6. V. B. Siramshetty, J. Nickel, C. Omieczynski, B. O. Gohlke, M. N. Drwal and R. Preissner, *Nucleic Acids Res*, 2016, **44**, D1080-1086.

7. M. B. Esch, T. L. King and M. L. Shuler, *Annual Review of Biomedical Engineering, Vol 13*, 2011, **13**, 55-72.

8. M. A. Lancaster and J. A. Knoblich, *Science*, 2014, **345**, 1247125.

9. X. L. Yin, B. E. Mead, H. Safaee, R. Langer, J. M. Karp and O. Levy, *Cell Stem Cell*, 2016, **18**, 25-38.

10. W. Y. Q., W. H., D. P.W., T. T. T., L. H. T., W. S., C. W. W. and Q. J. H., *ACS biomaterials science & engineering*, 2020, **6**, 5734-5743.

11. Y. J. Zhu, L. Wang, H. Yu, F. C. Yin, Y. Q. Wang, H. T. Liu, L. Jiang and J. H. Qin, *Lab on a Chip*, 2017, **17**, 2941-2950.

View Article Online
DOI: 10.1039/D0LC00921K

12. Y. Wang, L. Wang, Y. Zhu and J. Qin, *Lab Chip*, 2018, **18**, 851-860.

13. H. Liu, Y. Wang, K. Cui, Y. Guo, X. Zhang and J. Qin, *Advanced Materials*, 2019, **31**.

14. S. N. Bhatia and D. E. Ingber, *Nature Biotechnology*, 2014, **32**, 760-772.

15. D. Huh, Y. S. Torisawa, G. A. Hamilton, H. J. Kim and D. E. Ingber, *Lab on a Chip*, 2012, **12**, 2156-2164.

16. J. P. Wikswo, *Future Sci OA*, 2017, **3**, FSO163.

17. Y. Wang, H. Wang, P. Deng, W. Chen, Y. Guo, T. Tao and J. Qin, *Lab Chip*, 2018, **18**, 3606-3616.

18. T. Tao, Y. Wang, W. Chen, Z. Li, W. Su, Y. Guo, P. Deng and J. Qin, *Lab Chip*, 2019, **19**, 948-958.

19. S. D. Sie, J. M. B. Wennink, J. J. van Driel, A. G. W. te Winkel, K. Boer, G. Casteelen and M. M. van Weissenbruch, *Archives of Disease in Childhood-Fetal and Neonatal Edition*, 2012, **97**, F472-F476.

20. K. A. Yonkers, K. L. Wisner, D. E. Stewart, T. F. Oberlander, D. L. Dell, N. Stotland, S. Ramin, L. Chaudron and C. Lockwood, *General Hospital Psychiatry*, 2009, **31**, 403-413.

21. Z. Li, L. Jiang, T. Tao, W. Su, Y. Guo, H. Yu and J. Qin, *Toxicol Res (Camb)*, 2017, **6**, 372-380.

22. F. Yin, Y. Zhu, M. Zhang, H. Yu, W. Chen and J. Qin, *Toxicol In Vitro*, 2019, **54**, 105-113.

23. Q. Wang, H. Yang, A. Bai, W. Jiang, X. Li, X. Wang, Y. Mao, C. Lu, R. Qian, F. Guo, T. Ding, H. Chen, S. Chen, J. Zhang, C. Liu and N. Sun, *Biomaterials*, 2016, **105**,

View Article Online
DOI: 10.1039/D0LC00921K

52-65.

24. F. C. Yin, Y. J. Zhu, Y. Q. Wang and J. H. Qin, *ACS Biomater. Sci. Eng.*, 2018, **4**, 1908-1915.

25. X. Lian, J. Zhang, S. M. Azarin, K. Zhu, L. B. Hazeltine, X. Bao, C. Hsiao, T. J. Kamp and S. P. Palecek, *Nat Protoc*, 2013, **8**, 162-175.

26. N. Huebsch, P. Loskill, M. A. Mandegar, N. C. Marks, A. S. Sheehan, Z. Ma, A. Mathur, T. N. Nguyen, J. C. Yoo, L. M. Judge, C. I. Spencer, A. C. Chukka, C. R. Russell, P. L. So, B. R. Conklin and K. E. Healy, *Tissue Eng Part C Methods*, 2015, **21**, 467-479.

27. A. Mathur, P. Loskill, K. Shao, N. Huebsch, S. Hong, S. G. Marcus, N. Marks, M. Mandegar, B. R. Conklin, L. P. Lee and K. E. Healy, *Sci Rep*, 2015, **5**, 8883.

28. C. Xu, L. Wang, Y. Yu, F. Yin, X. Zhang, L. Jiang and J. Qin, *Biomater Sci*, 2017, **5**, 1810-1819.

29. M. D. Bootman, K. Rietdorf, T. Collins, S. Walker and M. Sanderson, *Cold Spring Harb Protoc*, 2013, **2013**, 83-99.

30. C. Oleaga, A. Riu, S. Rothemund, A. Lavado, C. W. McAleer, C. J. Long, K. Persaud, N. S. Narasimhan, M. Tran, J. Roles, C. A. Carmona-Moran, T. Sasserath, D. H. Elbrecht, L. Kumanchik, L. R. Bridges, C. Martin, M. T. Schnepper, G. Ekman, M. Jackson, Y. I. Wang, R. Note, J. Langer, S. Teissier and J. J. Hickman, *Biomaterials*, 2018, **182**, 176-190.

31. M. Gex-Fabry, E. Haffen, G. Paintaud, P. Bizouard, D. Sechter, P. R. Bechtel and L. P. Balant, *Therapeutic Drug Monitoring*, 2000, **22**, 701-711.

View Article Online
DOI: 10.1039/D0LC00921K

476 32. P. G. J. ter Horst, J. H. Proost, J. P. Smit, M. T. Vries, L. de Jong-van de Berg and B.
477 Wilffert, *European Journal of Clinical Pharmacology*, 2015, **71**, 1493-1500.
478 33. S. H. Preskorn and G. S. Jerkovich, *J Clin Psychopharmacol*, 1990, **10**, 88-95.
479 34. A. Szegedi, H. Wetzel, M. Leal, S. Hartter and C. Hiemke, *J Clin Psychiatry*, 1996, **57**,
480 257-264.
481 35. D. M. Bers, *Nature*, 2002, **415**.
482 36. C. W. McAleer, A. Pointon, C. J. Long, R. L. Brighton, B. D. Wilkin, L. R. Bridges, N.
483 Narasimhan Sriram, K. Fabre, R. McDougall, V. P. Muse, J. T. Mettetal, A. Srivastava,
484 D. Williams, M. T. Schnepper, J. L. Roles, M. L. Shuler, J. J. Hickman and L. Ewart,
485 *Sci Rep*, 2019, **9**, 9619.
486 37. J. H. Sung, C. Kam and M. L. Shuler, *Lab Chip*, 2010, **10**, 446-455.
487

View Article Online
DOI: 10.1039/D0LC00921K

Figures and legends

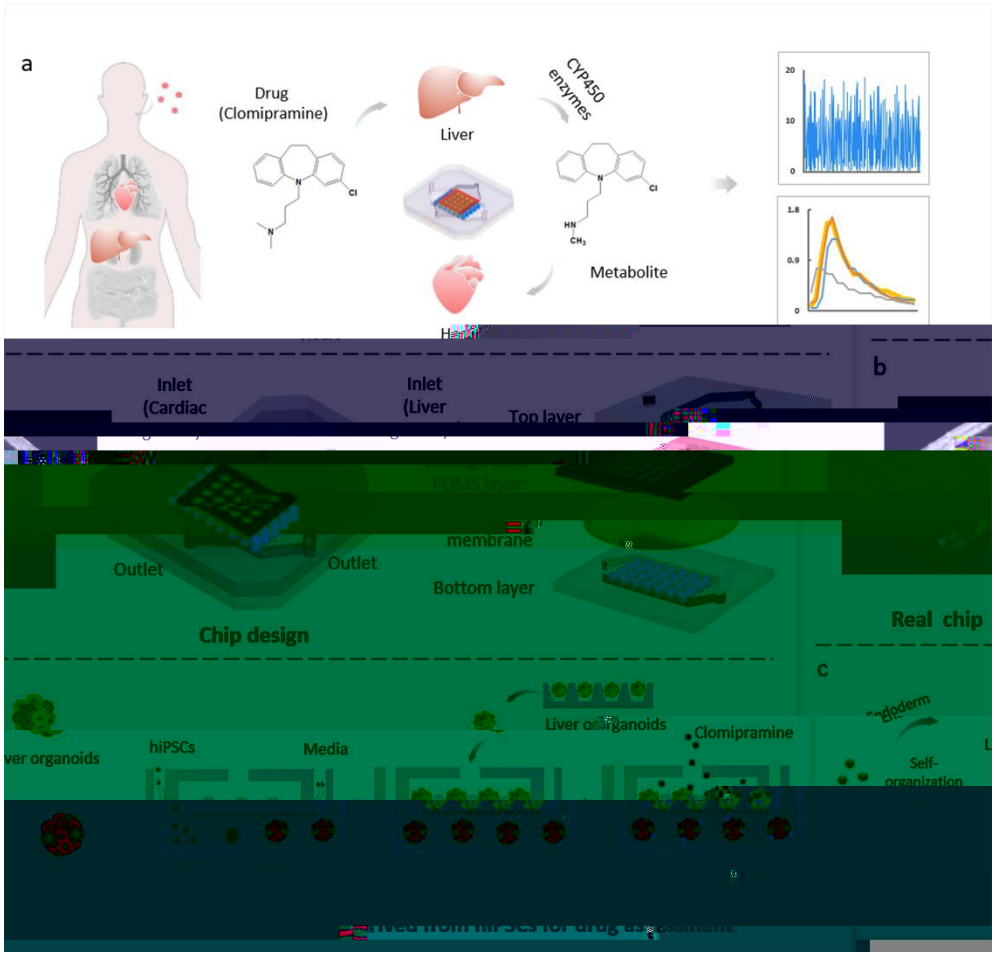

Figure 1. Illustration of the liver-heart organoids-on-chip for drug assessment of clomipramine. a, Schematic diagram of antidepressant drug clomipramine and its metabolites following liver metabolism *in vivo*. **b**, Design of multi-organoids-on-chip device, which consists of the top layer, through-hole PDMS layer, polycarbonate porous membrane and bottom layer. Self-organized liver organoids were cultured on the upper through-hole PDMS layer to form liver region, and cardiac organoids were cultured on the bottom micropillar layer to form heart region. **c,** The schematic overview of the experimental procedures. Heart organoids were formed by in situ differentiation and generation from hiPSCs on the bottom layer, and the day-20 hiPSC-derived liver organoids were then seeded into the top layer, thereby establishing the co-culture system of liver and heart organoids. Finally, this multi-organoids-on-chip was applied to assess toxicity of antidepressant drug in heart organoids.

View Article Online
DOI: 10.1039/D0LC00921K

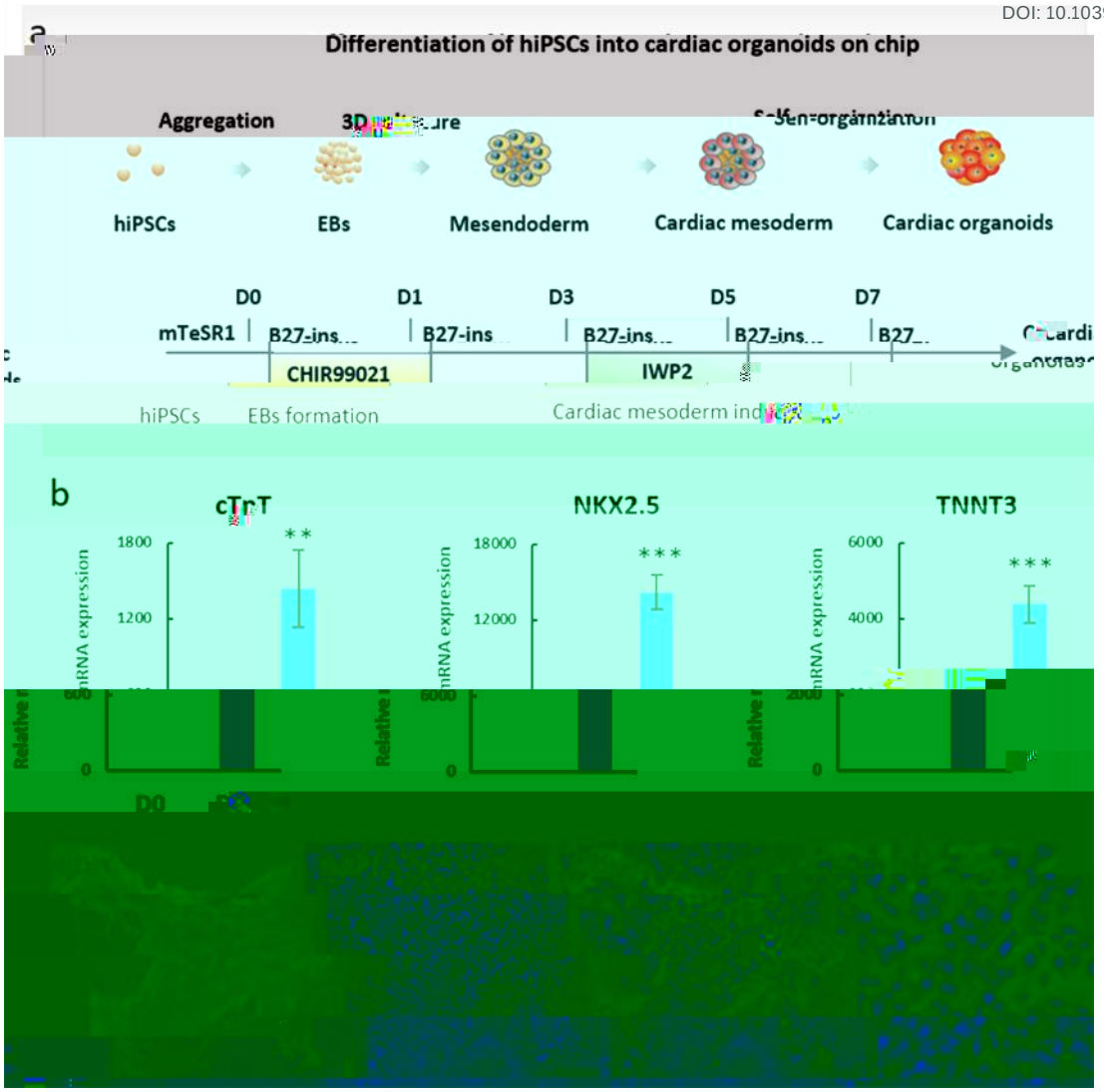

Figure 2. Characterization of hiPSC-derived cardiac organoids. a, The flow chart illustrates the process of the generation of heart organoids from hiPSCs. **b,** The relative mRNA expression of specific cardiac markers (cTnT, NKX 2.5, TNNT3) in day 20 cardiac organoids was quantified by real time-PCR, which were relative to that of day 0 hiPSCs. N=3 replicates, mean ± SD. (*, $P < 0.05$, **, $P < 0.01$, ***, $P < 0.001$). **c,** Immunohistochemistry analysis of cTnT in cardiac organoids on day 20. Scale bars, 100 μm.

View Article Online
DOI: 10.1039/D0LC00921K

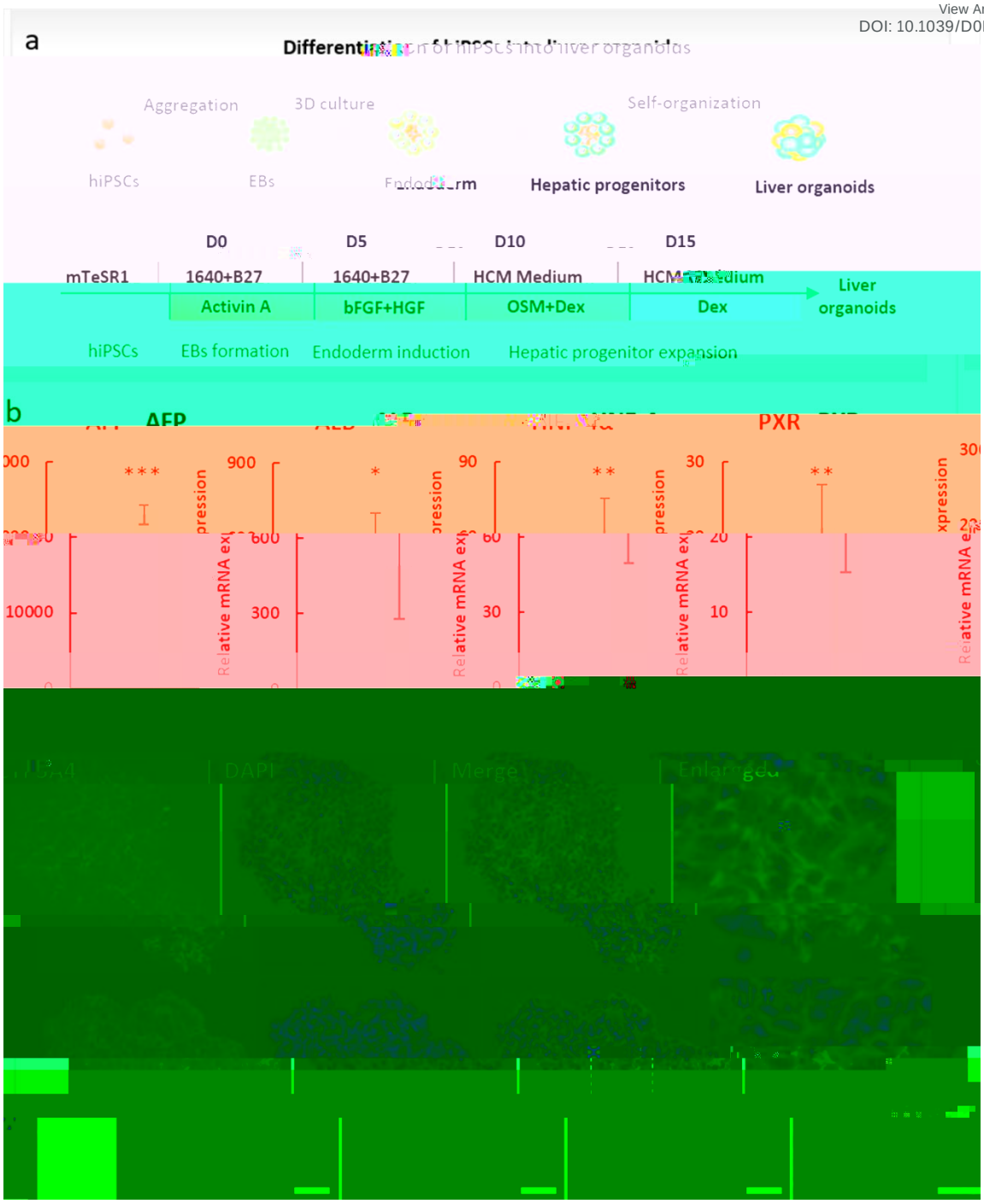

Figure 3. Characterization of hiPSC-derived liver organoids. a, The flow chart illustrates the process of the generation of hiPSC-derived liver organoids using a three-stage differentiation protocol. **b,** The hepatic progenitor (AFP), hepatocyte (ALB and HNF4α) and nuclear receptor (PXR) markers were quantified by real time-PCR in day 0 hiPSCs and day 20 liver organoids. N=3, mean ± SD. (*, $P < 0.05$, **, $P < 0.01$, ***, $P < 0.001$). **c,** Immunohistochemical staining of ALB and CYP450 enzyme marker (CYP3A4) in organoids on day 20. DAPI marks nuclei (blue). Scale bars, 50 μm.

View Article Online
DOI: 10.1039/D0LC00921K

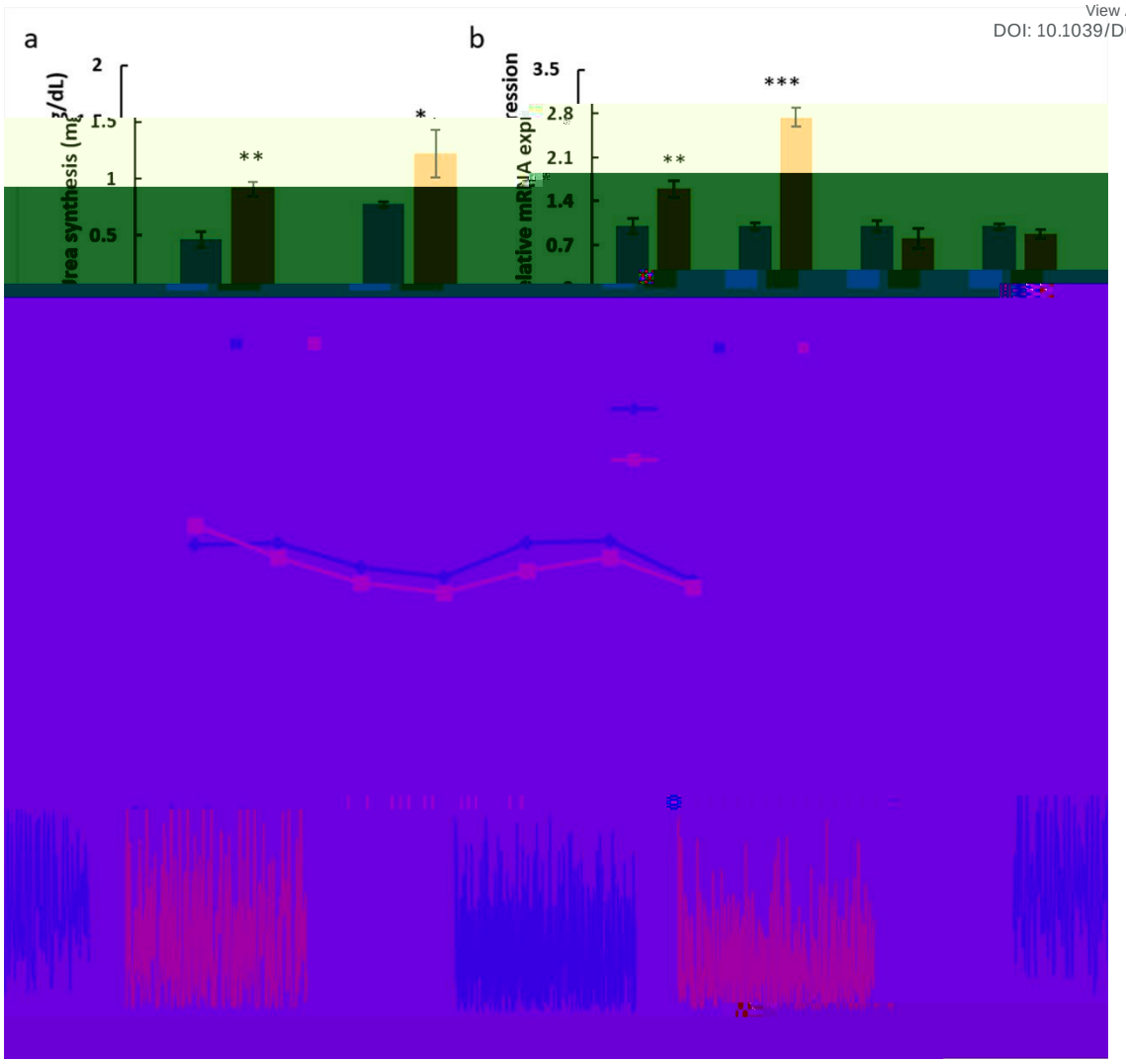

Figure 4. Characterization of the co-cultured human liver organoids and heart organoids on chip. a, Urea synthesis was quantified in liver organoids with (co-liver) or without (liver) cardiac tissues cultures on chip at 3 and 6 days. **b,** The mRNA expression of liver-specific metabolic enzymes (CYP3A4, CYP1A2, CYP2C19 and CYP2D6) in liver organoids with (co-liver) or without (liver) cardiac tissues coculture on chip was quantified by real time-PCR. N=3, mean ± SD. (*, $P < 0.05$, **, $P < 0.01$, ***, $P < 0.001$). **c-d,** Analysis of cardiac functional parameters: beat frequency **(c)** and beating velocity (μm/s) **(d)** in the presence or absence of liver organoids at different time points.

View Article Online
DOI: 10.1039/D0LC00921K

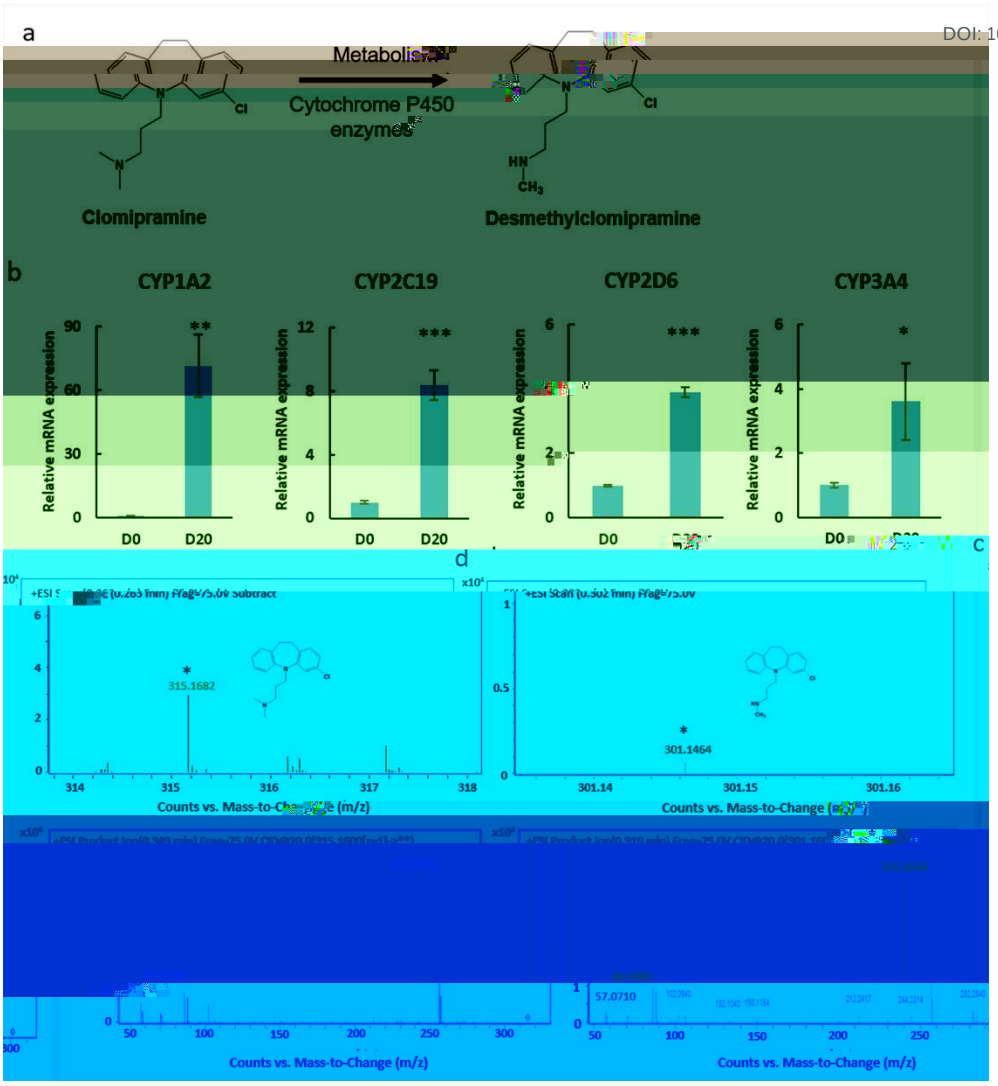

Figure 5. Identification of clomipramine and its metabolite (desmethylclomipramine) by liver organoids on the chip. a, The main metabolic process of clomipramine *in vivo*. **b,** The expression of metabolic enzyme genes (CYP1A2, CYP3A4, CYP2C19 and CYP2D6) were evaluated by real time-PCR in day 0 hiPSCs and day 20 liver organoids. N=3, mean ± SD. (*, $P < 0.05$, **, $P < 0.01$, ***, $P < 0.001$). **c-d**, Mass spectrum of clomipramine (**c**) and its metabolite (desmethylclomipramine) (**d**) (top) and the secondary mass spectrogram (bottom) from the supernatants of liver organoids with 1μM clomipramine treatment for 24 h using LC-MS (liquid chromatography mass spectrometry) technology.

View Article Online
DOI: 10.1039/D0LC00921K

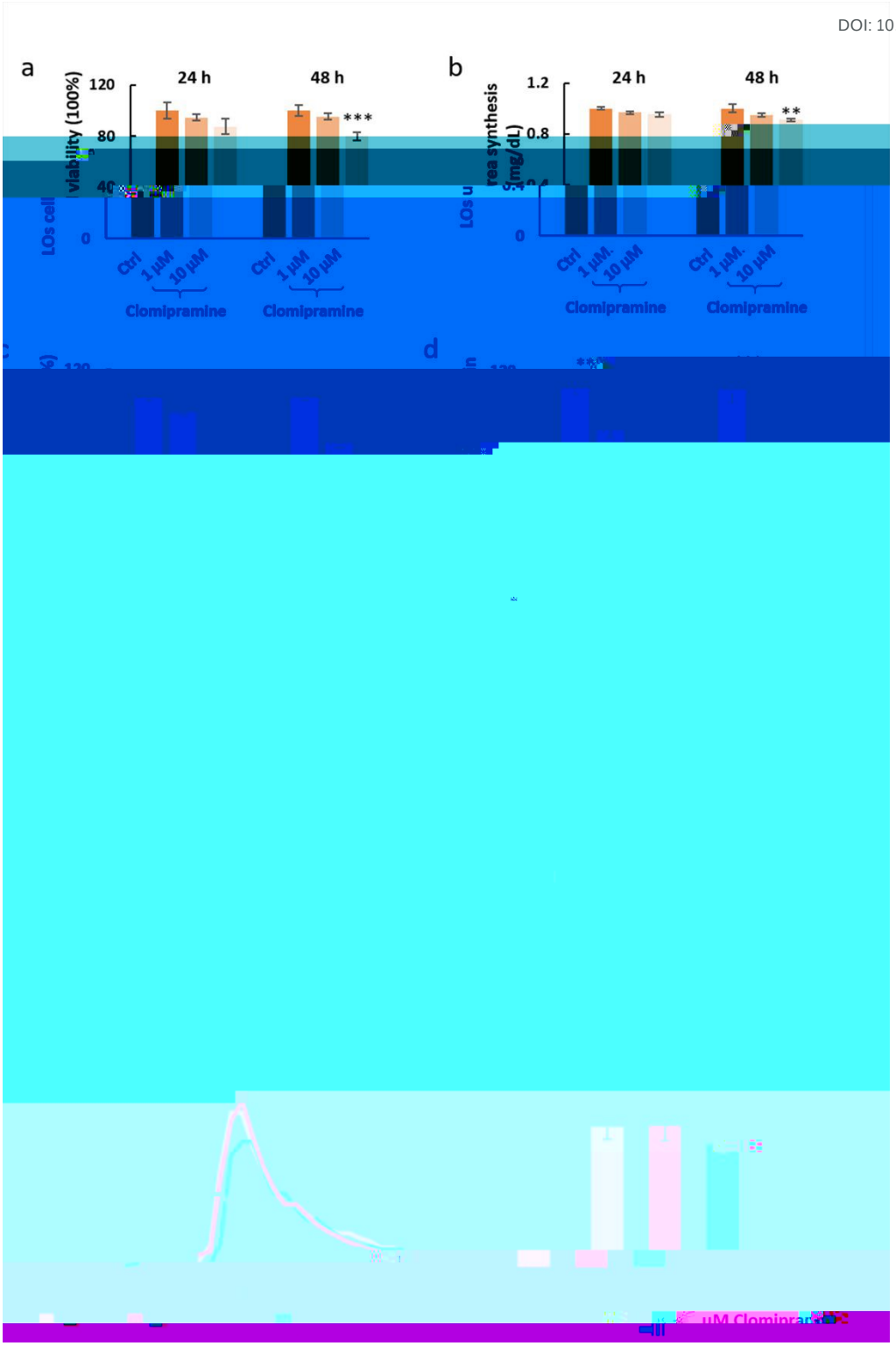

Figure 6. Assessment of drug-induced cardiactoxicity after liver metabolism on the liver-heart organoids-on-chip. a, Quantitative analysis of cell viability in liver organoids on day 20 after treatment with clomipramine (1 μM and 10 μM) for 24 and 48 h. The cell viability was analyzed using CCK-8 kit. **b,** Identification of the urea synthesis in liver organoids after treatment with different concentrations of

clomipramine for 24 and 48 h. N=3, mean ± SD. **c-d,** Cell viability (**c**) and the beating rate (**d**) of the cardiac tissues were evaluated with clomipramine (1 μM) treatment for 24 h and 48 h in the presence and absence of liver organoids. N=3, mean ± SD. (*, $P < 0.05$, **, $P < 0.01$, ***, $P < 0.001$). **e,** Beating motion track of cardiac organoids with different treatments and the quantification of mean beating velocity of each group (N=3, mean ± SD. *, $P < 0.05$, **, $P < 0.01$, ***, $P < 0.001$). **f,** Fluorescence calcium imaging of hiPSC-COs under different treatment conditions and the quantification of the peak value of RFI. $F/F_0=(F_t-F_0)/F_0$, where F_t was the fluorescent intensity values of each frames and F_0 was the lowest fluorescence value. RFI: Relative fluorescence intensity. Scale bars, 200 μm. (N=6, mean ± SD.*, $P < 0.05$, **, $P < 0.01$, ***, $P < 0.001$).